FOUNDATIONS
ADVANCES

Volume 74 (2018)

Supporting information for article:

Ab initio structure determination and quantitative disorder analysis on nanoparticles by electron diffraction tomography

Yaşar Krysiak, Bastian Barton, Bernd Marler, Reinhard B. Neder and Ute Kolb

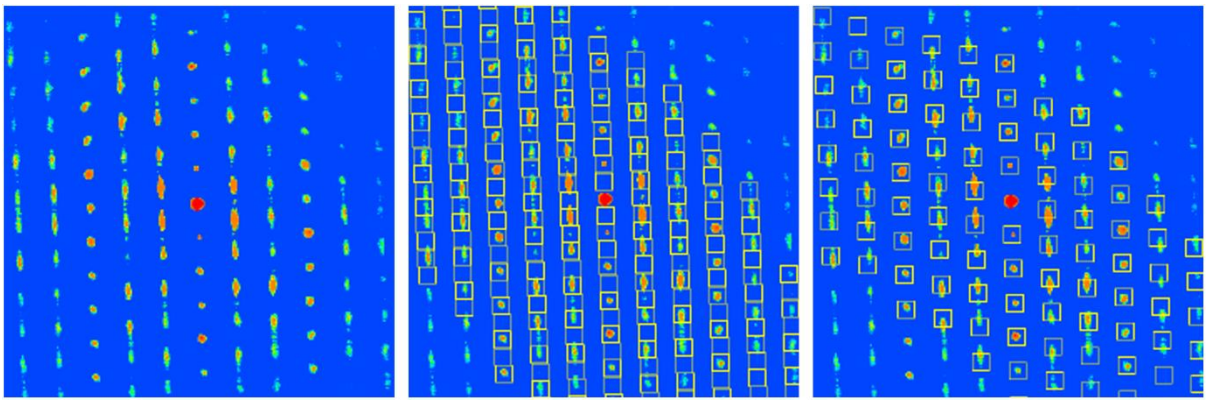

Figure S1 Visualisation of one recorded frame from stack oriented approx. along $[001]_{tetr}$. Yellow boxes show the integrated areas calculated from the determined BEA (b) and BEB (c) lattice.

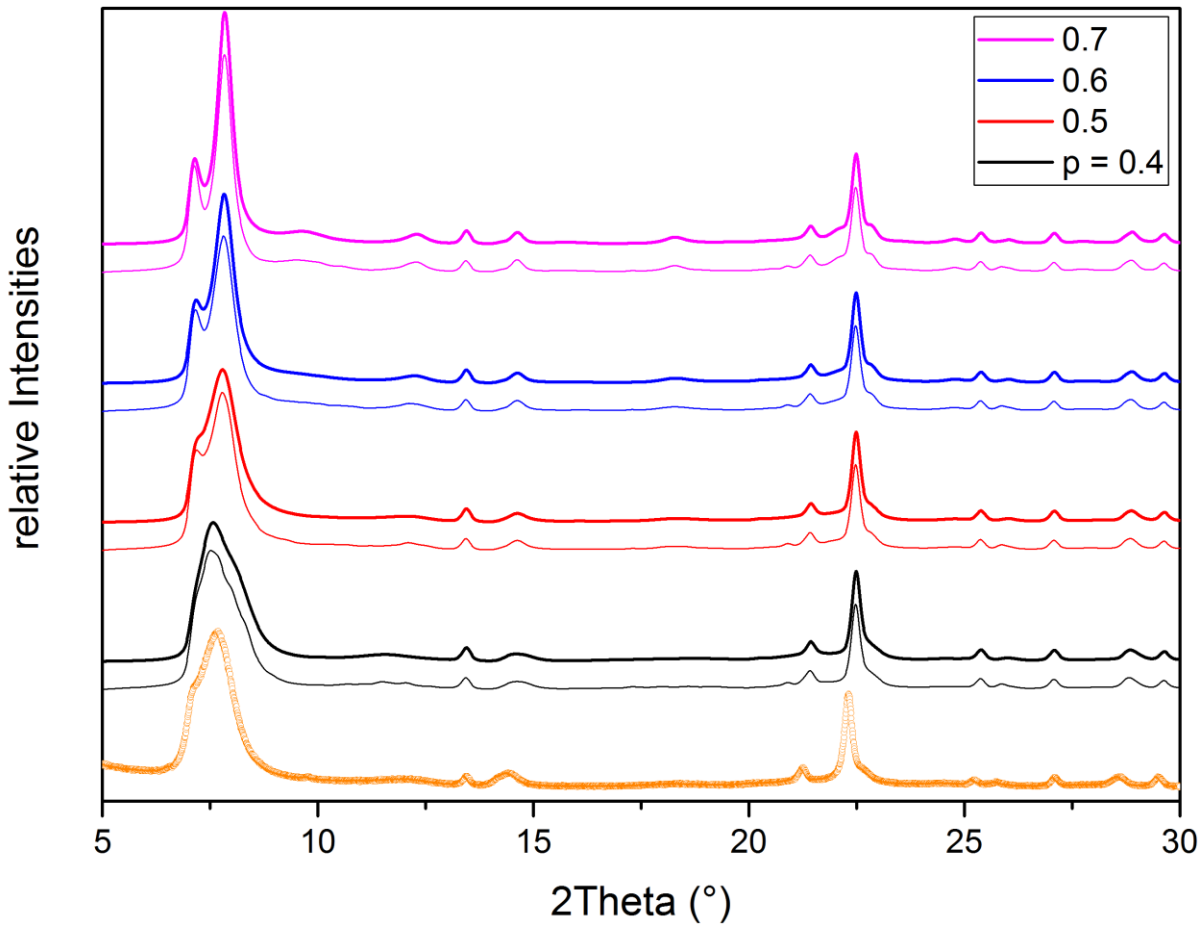

Figure S2 Comparison of powder patterns simulated with DIFFaX and DISCUS for different ratios of polymorph A and polymorph B. For each pair the DIFFaX pattern is the lower and the DISCUS pattern the upper curve. The curves have been offset along the vertical axis for clarity.

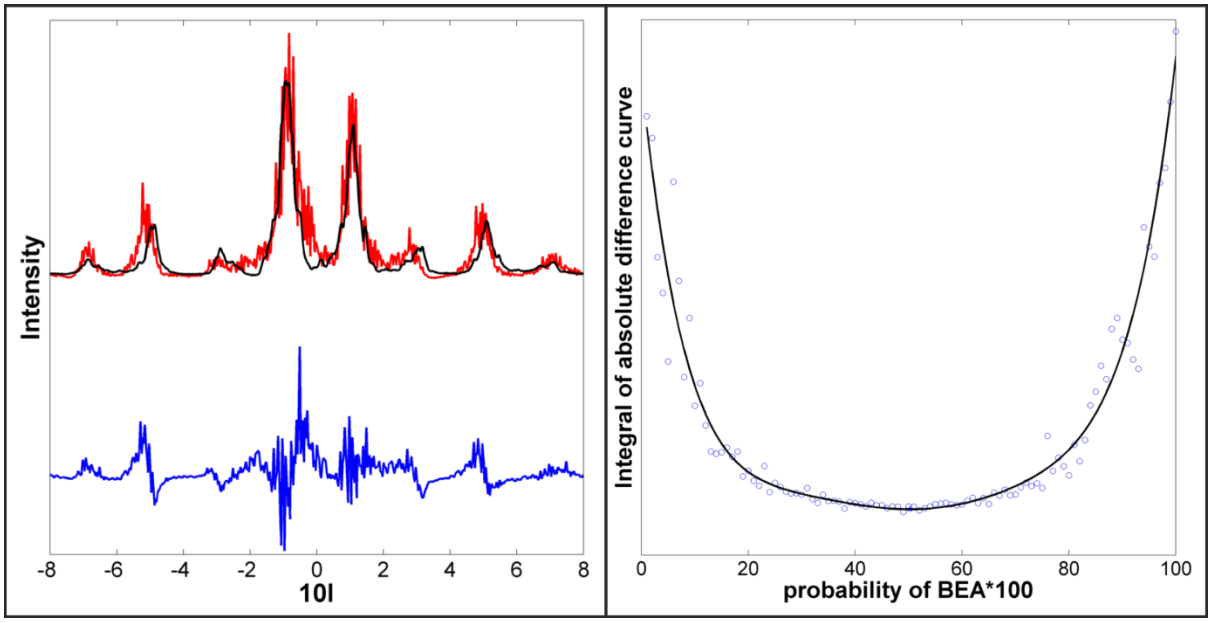

Figure S3 (a) Plot of the integrated absolute difference between simulated and experimental line profile taken along 10l against stacking probability for zeolite beta polymorph A. (b) Plot of experimental line profile 10l (black) and the simulated line profile 10l (red) of the stacking probability p = 0.48 and the corresponding difference curve (blue). The high frequency oscillations of the calculated profile are a Fourier artefact due the limited extend of the crystal.

Table S1 Atom positions of the refined structure solutions of BEA and BEB polymorphs.

BEA - zeolite beta polymorph A ($P4_122$)						**BEB - zeolite beta polymorph B ($C2/c$)**					
Label	Atom	x	y	z	U_{iso} (Å²)	Label	Atom	x	y	z	U_{iso} (Å²)
SI1	Si	0.665(3)	0.196(3)	0.555(1)	0.09(1)	SI1	Si	0.298(1)	0.704(1)	0.889(2)	0.078(7)
SI2	Si	0.957(3)	0.200(3)	0.447(1)	0.09(1)	SI2	Si	0.103(1)	0.515(1)	0.885(2)	0.074(7)
SI3	Si	0.959(3)	0.464(3)	0.445(1)	0.09(1)	SI3	Si	-0.033(1)	0.652(1)	0.881(2)	0.079(7)
SI4	Si	0.668(3)	0.460(2)	0.559(1)	0.08(1)	SI4	Si	0.336(1)	0.661(1)	1.110(2)	0.094(8)
SI5	Si	0.536(3)	0.536(3)	0.3750	0.12(2)	SI5	Si	0.0000	0.786(2)	0.7500	0.09(1)
SI6	Si	0.713(3)	0.464(3)	0.442(1)	0.10(1)	SI6	Si	0.084(1)	0.667(1)	1.116(2)	0.087(7)
SI7	Si	0.867(3)	0.538(3)	0.628(1)	0.13(2)	SI7	Si	0.196(1)	0.418(1)	1.242(2)	0.103(8)
SI8	Si	0.713(2)	0.199(3)	0.441(1)	0.08(1)	SI8	Si	0.216(2)	0.535(1)	1.112(2)	0.108(9)
SI9	Si	0.871(3)	0.129(3)	0.6250	0.08(2)	SI9	Si	0.0000	0.616(2)	1.2500	0.11(1)
O1	O	0.655(5)	0.170(5)	0.496(2)	0.09(1)	O1	O	0.167(2)	0.503(2)	1.004(2)	0.054(8)
O2	O	1.0000	0.17(1)	0.5000	0.13(3)	O2	O	0.002(2)	0.667(2)	1.003(2)	0.070(9)
O3	O	0.623(6)	0.526(7)	0.406(3)	0.16(3)	O3	O	0.232(2)	0.479(2)	1.193(2)	0.074(9)
O4	O	0.659(4)	0.324(4)	0.563(2)	0.08(1)	O4	O	0.431(2)	0.676(2)	1.187(3)	0.10(1)
O5	O	1.0000	0.486(6)	0.5000	0.07(2)	O5	O	0.327(2)	0.670(2)	0.998(3)	0.09(1)

O6	O	0.765(5)	0.517(5)	0.590(2)	0.10(2)	O6	O	-0.013(2)	0.725(2)	0.835(3)	0.10(1)
O7	O	0.768(4)	0.138(5)	0.589(2)	0.09(2)	O7	O	-0.111(2)	0.628(2)	0.836(3)	0.10(1)
O8	O	0.820(6)	0.181(5)	0.434(2)	0.11(2)	O8	O	0.303(2)	0.591(2)	1.130(3)	0.10(1)
O9	O	0.666(4)	0.483(4)	0.500(2)	0.06(1)	O9	O	0.034(2)	0.577(2)	0.865(3)	0.09(1)
O10	O	0.830(5)	0.479(4)	0.437(2)	0.09(2)	O10	O	0.220(2)	0.753(2)	0.869(3)	0.09(1)
O11	O	0.631(6)	0.144(6)	0.404(2)	0.15(2)	O11	O	0.143(3)	0.747(3)	1.123(3)	0.12(1)
O12	O	0.987(5)	0.339(6)	0.436(2)	0.13(2)	O12	O	0.137(3)	0.594(2)	1.131(3)	0.12(1)
O13	O	0.572(6)	0.151(6)	0.577(2)	0.16(2)	O13	O	0.042(3)	0.667(2)	1.191(3)	0.13(1)
O14	O	0.934(6)	0.530(7)	0.591(3)	0.18(3)	O14	O	0.159(3)	0.547(3)	0.836(4)	0.17(2)
O15	O	0.703(5)	0.330(6)	0.440(2)	0.13(2)	O15	O	0.067(3)	0.450(3)	0.835(4)	0.16(2)
O16	O	1.036(5)	0.137(5)	0.408(2)	0.12(2)	O16	O	0.249(3)	0.636(3)	0.824(4)	0.16(2)
O17	O	0.565(5)	0.515(6)	0.583(2)	0.11(2)						